THE JOURNAL OF BIOLOGICAL CHEMISTRY VOL. 288, NO. 14, pp. 9779–9789, April 5, 2013
© 2013 by The American Society for Biochemistry and Molecular Biology, Inc. Published in the U.S.A.

High Resolution Characterization of Myosin IIC Protein Tailpiece and Its Effect on Filament Assembly[S]

Received for publication, October 23, 2012, and in revised form, February 13, 2013 Published, JBC Papers in Press, February 20, 2013, DOI 10.1074/jbc.M112.430173

Masha M. Rosenberg[‡1], **Daniel Ronen**[§1], **Noa Lahav**[‡], **Elvira Nazirov**[§], **Shoshana Ravid**[§2], **and Assaf Friedler**[‡3]

From the [‡]*Institute of Chemistry, The Hebrew University of Jerusalem, Safra Campus Givat Ram, Jerusalem 91904 and the* [§]*Department of Biochemistry and Molecular Biology, The Institute for Medical Research Israel-Canada, The Hebrew University-Hadassah Medical School, Jerusalem 91120, Israel*

Background: NMII-C tailpiece positively charged region binds to the coiled-coil rod, inducing filament assembly.
Results: Positive and aromatic residues within the tailpiece are important for filament assembly, and the tailpiece binding sites in the rod were identified.
Conclusion: Specific amino acid residues within the tailpiece interact with multiple sites in the rod.
Significance: Understanding NMII filament assembly mechanism is crucial for exploring NMII based-cellular processes.

The motor protein nonmuscle myosin II (NMII) must undergo dynamic oligomerization into filaments to perform its cellular functions. A small nonhelical region at the tail of the long coiled-coil region (tailpiece) is a common feature of all dynamically assembling myosin II proteins. This tailpiece is a key regulatory domain affecting NMII filament assembly properties and is subject to phosphorylation *in vivo*. We previously demonstrated that the positively charged region of the tailpiece binds to assembly-incompetent NMII-C fragments, inducing filament assembly. In the current study, we investigated the molecular mechanisms by which the tailpiece regulates NMII-C self-assembly. Using alanine scan, we found that specific positive and aromatic residues within the positively charged region of the tailpiece are important for inducing NMII-C filament assembly and for filament elongation. Combining peptide arrays with deletion studies allowed us to identify the tailpiece binding sites in the coiled-coil rod. Elucidation of the mechanism by which the tailpiece induces filament assembly permitted us further investigation into the role of tailpiece phosphorylation. Sedimentation and CD spectroscopy identified that phosphorylation of Thr^{1957} or Thr^{1960} inhibited the ability of the tailpiece to bind the coiled-coil rod and to induce NMII-C filament formation. This study provides molecular insight into the role of specific residues within the NMII-C tailpiece that are responsible for shifting the oligomeric equilibrium of NMII-C toward filament assembly and determining its morphology.

Nonmuscle myosin II (NMII)[4] is an important motor protein that is ubiquitously expressed by all cell types. NMII mediates cellular activities that require contractility such as cytokinesis and motility (1–4). The basic unit of NMII is a hexamer composed of two identical heavy chains and two sets of light chains (see Fig. 1*A*) (5, 6). Each heavy chain includes an N-terminal globular head containing the force-generating domain and a C-terminal α-helical domain terminating in a small disordered tailpiece domain. Two α-helices wrap around each other within each hexamer to form an extended coiled-coil (5). Each NMII hexamer unit must further undergo dynamic oligomerization into filaments to perform its cellular functions (5). Therefore, the process of filament assembly is in equilibrium between inactive hexamers and active filaments. This equilibrium is an important regulatory step used by the cell to control NMII function. The factors influencing NMII filament assembly are divided into intrinsic factors derived from the properties of specific domains in the α-helix and extrinsic factors such as phosphorylation and protein-protein interactions (7, 8). All residues along the α-helix create charge periodicity, thereby facilitating the winding of two NMII molecules into a coiled-coil and promoting higher order oligomerization. In addition, two small assembly competence domains and a stretch of positively charged residues located at the C terminus of the coiled-coil are crucial for filament assembly (9–14). The α-helix is broken by a proline residue at the extreme C terminus of NMII, creating a small nonhelical tailpiece (see Fig. 1*A*). This tailpiece is a key regulatory domain that affects NMII filament assembly properties (15, 16) and *in vivo* function (15, 17–19) by interacting with the coiled-coil rod (16). These fundamental properties are further modulated by the cell to dynamically control the assembly-disassembly equilibrium of NMII (8). The globular head at the N terminus and the unstructured tailpiece at the C terminus are the two main regions crucial for this dynamic behavior. Activating the motor head, by light chain phosphorylation, results in increased filament assembly due to increased actin binding (8). In contrast, phosphorylation of the tailpiece results in filament disassembly in a previously unknown mechanism (8).

Mammalians have three NMII isoforms (NMII-A, NMII-B, and NMII-C) with 64–80% overall sequence identity. The three isoforms perform distinctive cellular functions, although some redundancy is observed. Recently, we showed that the NMII-C tailpiece is composed of two regions of opposite charge

[S] This article contains supplemental Table 1 and Figs. 1 and 2.
[1] Both authors contributed equally to this work.
[2] The Dr. Daniel G. Miller Chair in Cancer Research. To whom correspondence may be addressed. E-mail: shoshr@ekmd.huji.ac.il.
[3] Supported by a starting grant from the European Research Council under the European Community Seventh Framework Programme (FP7/2007-2013)/ERC Grant 203413. To whom correspondence may be addressed. E-mail: assaf.friedler@mail.huji.ac.il.
[4] The abbreviations used are: NMII, nonmuscle myosin II; tailpiece, nonhelical tailpiece; pT, phospho-threonine; Fmoc, *N*-(9-fluorenyl)methoxycarbonyl.

(see Fig. 1*A*) (16). The N-terminal region of the tailpiece (residues 1946–1967) has a net positive charge of +7, whereas its C-terminal region (residues 1968–2000) has a net negative charge of −10 (see Fig. 1*A*) (16). We further showed that the positively charged region binds to assembly-incompetent NMII-C fragments, inducing filament assembly, and that the negatively charged region is responsible for NMII paracrystal morphology (16). In the current study, we further investigated the mechanism by which the positive part of the tailpiece regulates filament formation. We show that positive and aromatic residues within the positively charged region of the tailpiece (residues 1946–1967) are important for NMII-C filament assembly. Furthermore, we identified tailpiece binding sites in the coiled-coil rod and demonstrate the effect of phosphorylation on the ability of the tailpiece to bind the coiled-coil rod.

EXPERIMENTAL PROCEDURES

Peptide Synthesis, Labeling, and Purification—Tailpiece peptides and the control peptide KKLANAPRRLKKNSS, bearing a positive charge of +6, were synthesized using the Liberty microwave-assisted peptide synthesizer (CEM Corp.) using standard Fmoc chemistry. The protected phospho-threonine derivative Fmoc-Thr(HPO_3Bzl)-OH was ordered from Chem-Impex. The coupling and deprotection of the phospho-Thr amino acid were carried out at room temperature because the benzyl protecting group may dissociate at a high temperature. Tryptophan was added to the N termini of the peptides for determining their concentrations using UV spectroscopy. His tag was added to the N termini of several peptides used in the peptide array experiments. The peptides were cleaved from the resin by shaking in a mixture of 92% TFA, 5% triple distilled water, and 3% triisopropylsilane at room temperature for 4 h. Peptide purification was performed using a Gilson HPLC equipped with a reverse-phase C8 semipreparative column (Advanced Chromatography Technologies) with a gradient of 5–60% acetonitrile in water (both containing 0.1% v/v trifluoroacetic acid). Peptide identity and purity were determined by MALDI-TOF mass spectrometry and analytical HPLC. Peptide concentration was determined using a UV spectrophotometer (Shimadzu Kyoto, Japan).

Construction of NMII-C Rod Mutants—NMII-C accession number AY363100 was used for this study. IIC-$Rod_{1296-1854}$ was constructed as described (16). IIC-$Rod_{1296-1854}$ internal deletions were created by introducing two SalI sites by consecutive rounds of site-directed mutagenesis, using the QuikChange II kit (Stratagene, La Jolla, CA) according to the manufacturer's protocol. The resulting plasmid was digested with SalI and self-ligated. A third round of site-directed mutagenesis was then performed to restore the original residue to the rod. All plasmids were confirmed by Sanger sequencing. Site-directed mutagenesis was performed using the following primers: $SalI^{1494}$, forward, 5′-GTG GAA GAC CGT GAA CGT CGA CAG GCC GAA GGC CGG G-3′; reverse, 5′-CCC GGC CTT CGG CCT GTC GAC GTT CAC GGT CTT CCA C-3′; $SalI^{1578}$, forward, 5′-GGA GGA TGA GCT GAC AGG TCG ACA GGA TGC CAA GCT GCG C-3′; reverse, 5′-GCG CAG CTT GGC ATC CTG TCG ACC TGT CAG CTC ATC CTC C-3′; IIC-$Rod_{1296-1854}^{\Delta 1494-1578}$ SalI removal, forward, 5′-CTG TGG AAG ACC GTG AAC GGG CAG AGG ATG CCA AGC TGC G-3′; reverse, 5′-CGC AGC TTG GCA TCC TCT GCC CGT TCA CGG TCT TCC ACA G-3′; $SalI^{1663}$, forward, 5′-CTG CTG GGC AGG GCA AGG AAG GTC GAC TGA AGC AGC TGA AG-3′; reverse, 5′-CTT CAG CTG CTT CAG TCG ACC TTC CTT GCC CTG CCC AGC AG-3′; IIC-$Rod_{1296-1854}^{\Delta 1579-1663}$ SalI removal, forward, 5′-GGA TGA GCT GAC AGC CGC AGT GAA GCA GCT GAA GAA GAT GC-3′; reverse, 5′-GCA TCT TCT TCA GCT GCT TCA CTG CGG CTG TCA GCT CAT CC-3′; $SalI^{1748}$, forward, 5′-GCA ATC TTA GCA AGG CAG GTC GAC TGG AGG AAA AAC GGC AGC-3′; reverse, 5′-GCT GCC GTT TTT CCT CCA GTC GAC CTG CCT TGC TAA GAT TGC-3′; IIC-$Rod_{1296-1854}^{\Delta 1664-1748}$ SalI removal, forward, 5′-GCA GGG CAA GGA AGA GAC CCT GGA GGA AAA ACG GCA GCT GG-3′; reverse, 5′-CCA GCT GCC GTT TTT CCT CCA GGG TCT CTT CCT TGC CCT GC-3′. IIC-$Rod_{1296-1854}^{\Delta 1466-1578}$ was created in a similar manner using the following primers: $SalI^{1466}$ forward, 5′-GCA AAG CAG CTC CTG AGC AGT CGA CGA GAA GAA GCA GCG G-3′; reverse, 5′-CCG CTG CTT CTT CTC GTC GAC TGC TCA GGA GCT GCT TTG C-3′; IIC-$Rod_{1296-1854}^{\Delta 1466-1578}$ SalI removal, forward, 5′-GCA AAG CAG CTC CTG AGC ACA GCA GAG GAT GCC AAG CTG CGC-3′; reverse, 5′-GCG CAG CTT GGC ATC CTC TGC TGT GCT CAG GAG CTG CTT TGC-3′. Assembly-competent rod constructs containing or lacking the tailpiece were generated using the same method and primers described above, performed on IIC-$Rod_{1296-2000}$ and IIC-$Rod_{1296-1955}$ described in Ref. 16.

Protein Expression and Purification—IIC-Rod proteins were expressed and purified as described (16, 20).

Sedimentation Assay—Samples of IIC-Rod fragments were mixed with peptides in 25 mM phosphate buffer, pH 7.2, and ionic strength of 150 mM at a 1:4 molar ratio. 500 μl of the sample mixes were incubated at room temperature for 4 h and then centrifuged at 100,000 × *g* for 1 h at 4 °C (Beckman TLA-120 rotor, 55,000 rpm). Following centrifugation, 450 μl of each sample were transferred to fresh tubes. The remainder of the supernatant was removed, and the pellet was dissolved in 500 μl of 25 mM phosphate buffer, pH 7.2, with ionic strength of 600 mM. Samples of the supernatants and of the dissolved pellets were analyzed using SDS-PAGE. The solubility of the IIC-$Rod_{1296-1854}$ (expressed as a percentage of the fragment in the supernatant) was determined by measuring the relative amount of each IIC-Rod fragment in the pellet and in the supernatant fractions by densitometry of the Coomassie Brilliant Blue-stained PAGE bands using Fujifilm image analyzer LAS-1000 Plus and the densitometry program Fujifilm Image Gauge version 3.4.

Negative Staining for Electron Microscopy—EM studies were performed as described (13, 20) with the following modifications. Filament formation was performed in a buffer containing 20 mM Tris, pH 7.5, ionic strength 116 mM with 12 mM $CaCl_2$ and 18 mM $MgCl_2$. An additional wash step was added after protein deposition on the grid for the electron microscopy experiments. Filament length was measured on at least 16 filaments from a minimum of six independent micrographs using

TABLE 1
NMH-C tailpiece peptides used in this study
Blue characters, positively charged residues; *red characters*, negatively charged residues; *bold characters*, residues that were substituted by alanine.

Peptide	Amino acid sequence
$Tailpiece_{1946-2000}$	WRNRLRRGPLTFTTRTVRQVFRLEEGVASDEEEAEGAEPGSAPGQEPEAPPPATPQ
$Tailpiece_{1946-1967}$	WRNRLRRGPLTFTTRTVRQVFRL
$Tailpiece_{1968-2000}$	WEEGVASDEEEAEGAEPGSAPGQEPEAPPPATPQ
R1946A	W**A**NRLRRGPLTFTTRTVRQVFRL
N1947A	WR**A**RLRRGPLTFTTRTVRQVFRL
R1948A	WRN**A**LRRGPLTFTTRTVRQVFRL
L1949A	WRNR**A**RRGPLTFTTRTVRQVFRL
R1950A	WRNRL**A**RGPLTFTTRTVRQVFRL
R1951A	WRNRLR**A**GPLTFTTRTVRQVFRL
G1952A	WRNRLRR**A**PLTFTTRTVRQVFRL
P1953A	WRNRLRRG**A**LTFTTRTVRQVFRL
L1954A	WRNRLRRGP**A**TFTTRTVRQVFRL
T1955A	WRNRLRRGPL**A**FTTRTVRQVFRL
F1956A	WRNRLRRGPLT**A**TTRTVRQVFRL
T1957A	WRNRLRRGPLTF**A**TRTVRQVFRL
T1958A	WRNRLRRGPLTFT**A**RTVRQVFRL
R1959A	WRNRLRRGPLTFTT**A**TVRQVFRL
T1960A	WRNRLRRGPLTFTTR**A**VRQVFRL
V1961A	WRNRLRRGPLTFTTRT**A**RQVFRL
R1962A	WRNRLRRGPLTFTTRTV**A**QVFRL
Q1963A	WRNRLRRGPLTFTTRTVR**A**VFRL
V1964A	WRNRLRRGPLTFTTRTVRQ**A**FRL
F1965A	WRNRLRRGPLTFTTRTVRQV**A**RL
R1966A	WRNRLRRGPLTFTTRTVRQVF**A**L
L1967A	WRNRLRRGPLTFTTRTVRQVFR**A**
$Tailpiece_{1946-1967-pT^{1957}}$	WRNRLRRGPLTF**pT**TRTVRQVFRL
$Tailpiece_{1946-1967-pT^{1960}}$	WRNRLRRGPLTFTTR**pT**VRQVFRL
Control peptide	WKKLANAPRRLKKNSS

ImageJ software calibrated to the scale bar. Statistical significance was determined using the Student's *t* test.

CD Measurements—Stock solutions of the peptides were prepared by dissolving the lyophilized peptides in 25 mM sodium phosphate buffer, pH 7.2, 100 mM NaCl. Solutions of $IIC\text{-}Rod_{1296-1854}$ in the presence and absence of each peptide were prepared by mixing stock solutions of each protein and peptide at 1:4 molar ratio. The final concentration of $IIC\text{-}Rod_{1296-1854}$ was 0.005 mM. CD spectra were recorded using a J-810 spectropolarimeter (JASCO) in a 0.1-cm quartz cuvette for far-ultraviolet CD spectroscopy. Far-ultraviolet CD spectra were collected over 190–260 nm at room temperature.

Peptide Array Screening—The peptide arrays were synthesized by INTAVIS Bioanalytical Instruments (21). The peptide array was immersed overnight in blocking solution containing 50 mM Tris·HCl, pH 7.5, 0.15 M NaCl, 0.1% Tween 20, and 5% sucrose and prewashed three times in Tris-buffered saline with Tween. Peptides in final concentration of 50 μM in blocking solution were incubated with the array for 1 h at room temperature followed by washing three times for 10 min with Tris-buffered saline with Tween. The binding was detected with anti-His tag-conjugated HRP, using a chemiluminescence blotting substrate SuperSignal reagent (Beit Haemek) according to the manufacturer's instructions.

RESULTS

Positive and Aromatic Residues in the Positively Charged Region of the Tailpiece Are Important for Mediating $IIC\text{-}Rod_{1296-1854}$ Filament Assembly—Understanding the interactions between the tailpiece and the coiled-coil rod at the molecular level is important for revealing the mechanism by which the tailpiece regulates NMII filament assembly. To identify the specific residues within the tailpiece that are responsible for its activity, alanine scan of all tailpiece residues was performed. We synthesized a series of peptides in which each residue in the positively charged region of the tailpiece was substituted by alanine and tested their effect on NMII-C rod filament assembly. Based on NMII-C $Tailpiece_{1946-1967}$ sequence, 22 alanine-substituted peptides were synthesized (Table 1). The effect of these peptides on NMII-C filament assembly was tested on a fragment of NMII-C coiled-coil lacking the C-terminal 146 residues ($IIC\text{-}Rod_{1296-1854}$, Fig. 1*B*). This fragment does not create filaments on its own even at low salt concentrations (16) but does so upon adding the WT $Tailpiece_{1946-1967}$ (16) (Fig. 2, *A* and *B*). Incubating $IIC\text{-}Rod_{1296-1854}$ with the $Tailpiece_{1946-1967}$ pep-

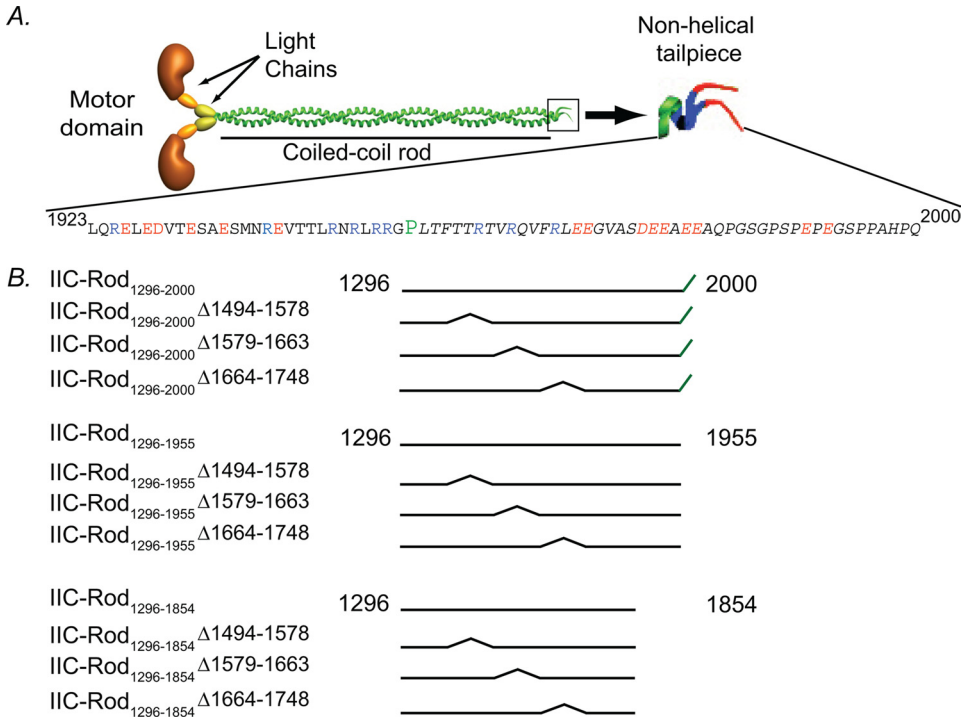

FIGURE 1. *A*, schematic representation of the NMII functional domains and the sequence of the nonhelical tailpiece. *Blue characters*, positively charged residues; *red characters*, negatively charged residues; *P in green*, proline. *B*, schematic presentation of IIC-Rod fragments used in this study. The *numbers* represent amino acid residue positions in the full-length protein.

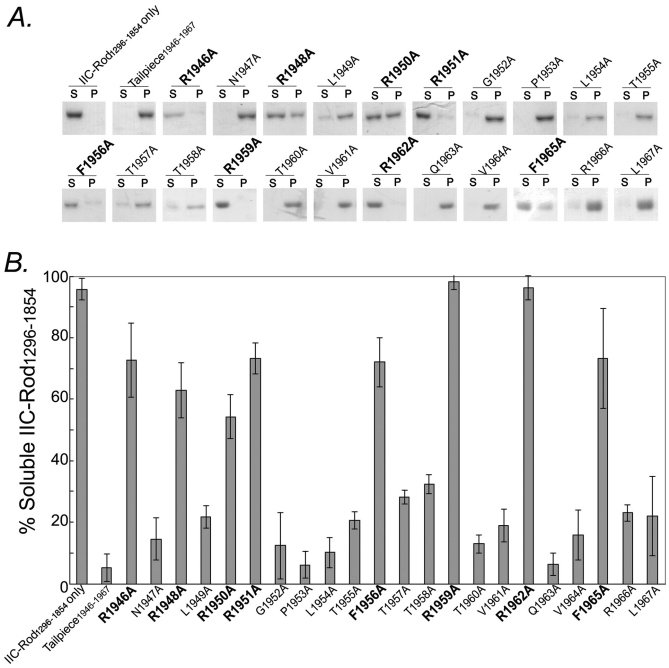

FIGURE 2. **Sedimentation of IIC-Rod$_{1296-1854}$ by alanine-substituted peptides derived from the positively charged region of the tailpiece.** *A*, 5 μM IIC-Rod$_{1296-1854}$ was incubated in the presence of 20 μM tailpiece peptides at ionic strength of 100 mM for 4 h at room temperature. Samples were centrifuged for 1 h at 100,000 $\times$ *g* at 4 °C. Equal amounts of supernatant and pellet were separated on SDS-PAGE and stained with Coomassie Blue. *S*, supernatant, *P*, pellet. *B*, fraction of soluble IIC-Rod$_{1296-1854}$ following incubation with alanine-substituted peptides. Alanine substitutions that show an effect on the activity of WT Tailpiece$_{1946-1967}$ are in *bold letters*. The results are averages $\pm$ S.D. of at least three independent experiments.

tides R1959A and R1962A completely abolished the tailpiece ability to induce filament assembly. Incubation of IIC-Rod$_{1296-1854}$ with the Tailpiece$_{1946-1967}$ peptides, R1946A, R1948A, R1950A, R1951A, F1956A, and F1965A, resulted in ~7-fold increase in solubility when compared with WT Tailpiece$_{1946-1967}$ (Fig. 2, *A* and *B*), demonstrating a major inhibition of tailpiece function. Substituting the remaining tailpiece residues to alanine had a markedly lower effect on filament assembly; however, even in this group, replacing T1957A or T1958A resulted in ~30% solubility, indicating that a residual effect on filament assembly was retained (Fig. 2, *A* and *B*). Taken together, these results point to the involvement of both the positive and the aromatic residues in the ability of the tailpiece to induce filament assembly because most of IIC-Rod$_{1296-1854}$ remained in the supernatant following ultracentrifugation. The observation that not all positive residues are important for binding suggests that the tailpiece effect may be due to a combination of specific electrostatic and hydrophobic interactions.

Using CD spectroscopy, we previously showed that IIC-Rod$_{1296-1854}$ alone adopts an α-helical conformation and that the addition of the positively charged Tailpiece$_{1946-1967}$ caused a decrease in α-helical content due to filament assembly (16). Supplemental Fig. 1*A* shows the CD spectra of the monomeric and paracrystalline states of IIC-Rod$_{1296-1954}$ achieved at high and low ionic strengths, respectively (15). At high ionic strength, this fragment displays a distinct α-helical conformation, whereas at low salt concentration, the α-helical content is decreased probably due to the formation of high order structures by coiled-coil monomers during filament assembly. We used CD spectroscopy to determine the effect of the

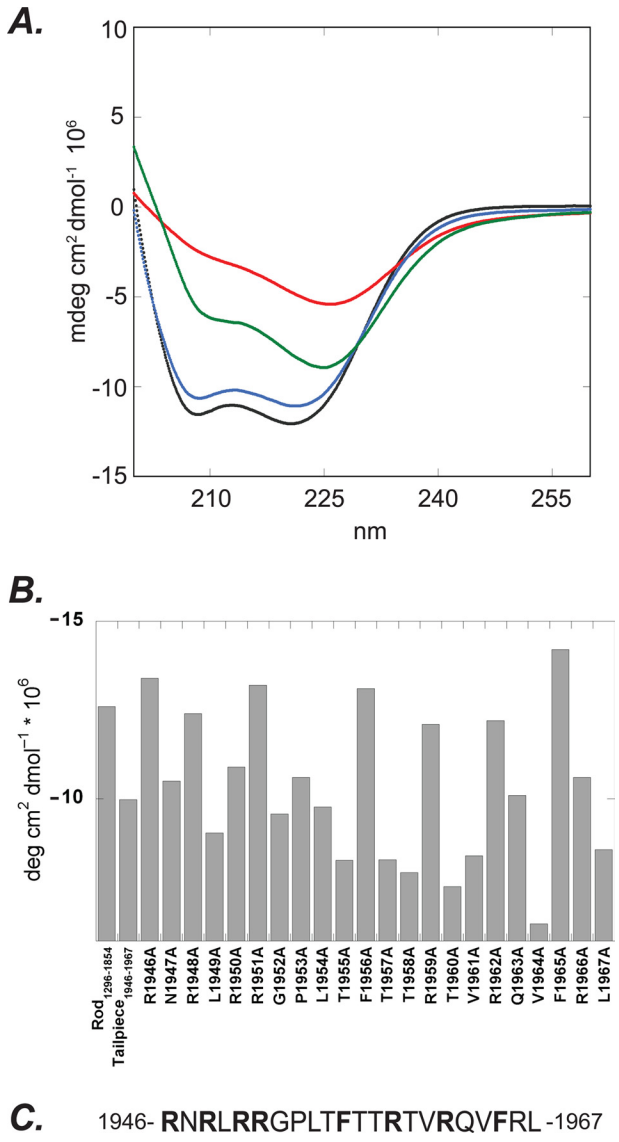

FIGURE 3. **CD spectra of IIC-Rod$_{1296-1854}$ in the presence of alanine-substituted peptides derived from the positively charged region of Tailpiece$_{1946-1967}$.** *A*, *black line*, IIC-Rod$_{1296-1854}$ alone; *red line*, with WT Tailpiece$_{1946-1967}$; *blue line*, with R1946A, which represents the group of alanine-substituted peptides that showed no effect on the coiled-coil structure of IIC-Rod$_{1296-1854}$ protein; *green line*, with G1952A, which represents the group of alanine-substituted peptides that showed an effect on the coiled-coil structure of IIC-Rod$_{1296-1854}$ protein. *deg*, degree. *B*, summary of CD intensities at 222 nm of 5 μM IIC-Rod$_{1296-1854}$ coiled-coil fragment recorded in the absence and in the presence of 20 μM alanine-substituted peptides derived from the positively charged region of Tailpiece$_{1946-1967}$. *mdeg*, millidegree. *C*, Tailpiece$_{1946-1967}$ peptide sequence. Alanine substitution of residues in *bold letters* showed no effect on the coiled-coil structure of IIC-Rod$_{1296-1854}$ protein, indicating their importance in filament assembly. The *numbers* represent amino acid residue positions in the full-length protein.

alanine-substituted peptides on the α-helical content of IIC-Rod$_{1296-1854}$. Peptides containing alanine substitutions at residues required for inducing IIC-Rod$_{1296-1854}$ filament assembly show smaller effect on the α-helical content of IIC-Rod$_{1296-1854}$ (Fig. 3 and supplemental Fig. 1*B*). However, alanine substitutions of residues that are not necessary for IIC-Rod$_{1296-1854}$ filament assembly decreased the α-helical content similar to wild type Tailpiece$_{1946-1967}$ (supplemental Fig. 1, *C* and *D*). These results further indicate that the positive and aromatic residues Arg^{1946}, Arg^{1948}, Arg^{1950}, Arg^{1951}, Arg^{1959}, Arg^{1962}, Phe^{1956}, and Phe^{1965} are important for mediating NMII-C filament assembly (Fig. 3*C*) and are in agreement with the sedimentation results.

Positive and Aromatic Residues in the Positive Region of the Tailpiece Are Important for NMII-C Paracrystal Formation—NMII filament assembly creates very organized defined structures, which are represented by large paracrystal filaments formed at low salt concentrations (13, 20). NMII-A and NMII-B rod fragments form paracrystals very similar to those formed by the full-length protein (13, 20, 22). Recently, we showed that this is also true for NMII-C as rod fragments create similar paracrystals to those created by fragments composed from the entire coiled-coil domain (15). As a result these, structures have been used to examine the capability of NMII to assemble into large filamentous structures (13, 20, 22). The ability of IIC-Rod$_{1296-1854}$ to form paracrystals was studied in the presence of the Tailpiece$_{1946-1967}$ peptides F1956A, R1959A, and R1966A. As expected IIC-Rod$_{1296-1854}$ alone was not capable of creating the distinctive long paracrystals of wild-type NMII-C, and only extremely small, needle-like structures were observed (Fig. 4*A*) (15). Adding the WT Tailpiece$_{1946-1967}$ to IIC-Rod$_{1296-1854}$ resulted in robust formation of long filamentous paracrystals (855.5 $\pm$ 238.4 nm) similar to those formed by WT NMII-C (Fig. 4 and supplemental Fig. 2). However, the addition of the R1959A peptide resulted in the formation of considerably shorter structures (279.05 $\pm$ 96.3 nm, $p = 9.1 \times 10^{-11}$) when compared with WT Tailpiece$_{1946-1967}$. R1966A substitution, on the other hand, had only a minimal effect on the length of filaments created (720.4 $\pm$ 279.0 nm, $p = 0.07$, Fig. 4 and supplemental Fig. 2). Substituting Phe^{1956} to alanine increased the filament length (1147.4 $\pm$ 430.5 nm, $p = 0.004$). Incubating IIC-Rod$_{1296-1854}$ with a control peptide bearing a net charge of +6 resulted in the formation of disordered aggregates only (Fig. 4). These results support the sedimentation and CD results, where the F1956A and R1959A substitutions significantly decreased the ability of the positive tailpiece peptide to induce filament formation, whereas R1966A has only a marginal effect (Figs. 2 and 3). The effect seems to alter the ability of IIC-Rod to elongate filaments rather than impair the initial assembly process.

Tailpiece$_{1946-1967}$ Binds IIC-Rod$_{1296-1854}$ at Several Regions—To identify the sites in IIC-Rod that interact with the positively charged region of the tailpiece, we designed an array composed of 94 partly overlapping peptides derived from residues 1271–1854 of IIC-Rod (supplemental Table 1). The peptides were designed based on the heptad repeat pattern of the coiled-coil (11, 22, 23). Each peptide is composed of 14 residues (two heptads) with an overlap of 7 residues. His-tagged tailpiece peptides were tested for their ability to bind the array. Tailpiece$_{1946-1967}$ bound several peptides derived from the IIC-Rod$_{1271-1854}$ sequence (Fig. 5*A* and Table 2), corresponding to six regions along IIC-Rod$_{1271-1854}$. These include residues 1348–1361, 1432–1480, 1544–1557, 1608–1642, and 1713–1775 (Table 2). These results indicate that the positively charged region of the tailpiece may interact with multiple sites within the NMII-C coiled-coil. Both the negative part of the tailpiece (Tailpiece$_{1968-2000}$) (Fig. 5*B*) and the full tailpiece

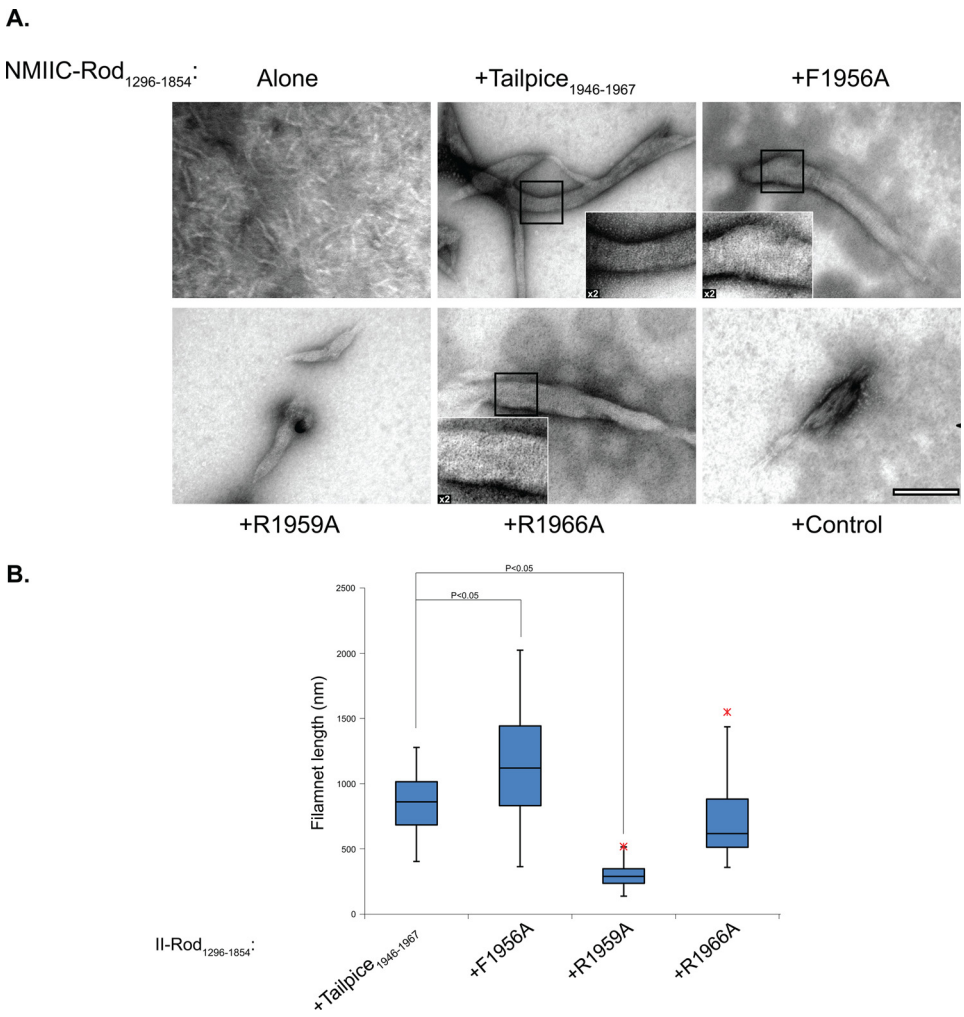

FIGURE 4. **The effect of the alanine-substituted peptides on IIC-Rod$_{1296-1854}$ paracrystal morphology.** *A*, IIC-Rod$_{1296-1854}$ was mixed with the different tailpiece peptides and control peptide at a 1:4 molar ratio in buffer (25 mM Tris buffer, 116 mM NaCl, 12 mM $CaCl_2$, and 18 mM $MgCl_2$). Filaments were negatively stained with uranyl acetate prior to viewing by transmission electron microscope at ×97000 as described under "Experimental Procedures." *Bar* represents 200 nm. *Insets* present a ×2 enlargement of presented figure, highlighting ordered striations in the paracrystals. *B*, box and whiskers plot indicating the length distribution of filament as quantified for the electron micrographs. The results are averages ± S.D. of at least three independent experiments.

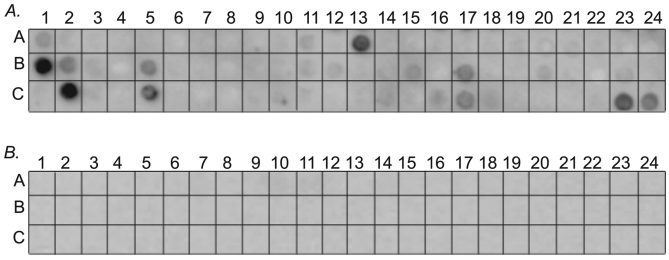

FIGURE 5. **Mapping of Tailpiece$_{1946-1967}$ binding site on IIC-Rod$_{1296-1854}$.** *A*, an array consisting of partly overlapping peptides derived from IIC-Rod$_{1296-1775}$ was screened for binding the positively charged Tailpiece$_{1946-1967}$ peptide. *B*, screening the peptide array for binding the negatively charged Tailpiece$_{1968-2000}$ peptide.

(Tailpiece$_{1946-2000}$, data not shown) did not interact with any peptide on the array. This is in agreement with our previous results, in which peptides containing the negatively charged region did not affect IIC-Rod$_{1296-1854}$ filament assembly (16).

To test whether the binding regions found in the peptide array screening (Fig. 5) play a role in filament assembly, we constructed assembly-incompetent IIC-Rod mutants lacking the putative internal binding sites (IIC-Rod$_{1296-1854}^{\Delta 1494-1578}$, IIC-Rod$_{1296-1854}^{\Delta 1579-1663}$, and IIC-Rod$_{1296-1854}^{\Delta 1664-1748}$, Figs. 1 and 6*A*) and tested the ability of Tailpiece$_{1946-1967}$ to induce filament assembly of these Rod deletions (Fig. 6). The deletions were in consecutive regions spanning 84 residues each. The rod constructs were designed to preserve the heptad repeat pattern to maintain the coiled-coil structure (11, 22, 23). All IIC-Rod$_{1296-1854}$ deletion mutants were unable to form filaments under normal conditions, similar to IIC-Rod$_{1296-1854}$

TABLE 2

IIC-Rod$_{1271-1954}$-derived peptides from the array that bound Tailpiece$_{1946-1967}$

Peptide array screening was performed as described under "Experimental Procedures." See text for details.

Peptide number	Binding residues	Sequence
A13	1348–1361	ETRAKLALGSRVRA
B1–2	1432–1452	KTEAVERLERARRRLQQELDD
B5	1460–1473	QKQLLSTLEKKQRK
B17	1544–1557	VGKNVHELERARKA
C2	1608–1621	GEERRRQLAKQLRD
C5	1629–1642	ERKQRALAMAARKK
C17	1713–1726	LQEELAASDRARRQ
C23–24	1755–1775	LEGRLSQLEEELEEEQNNSEL

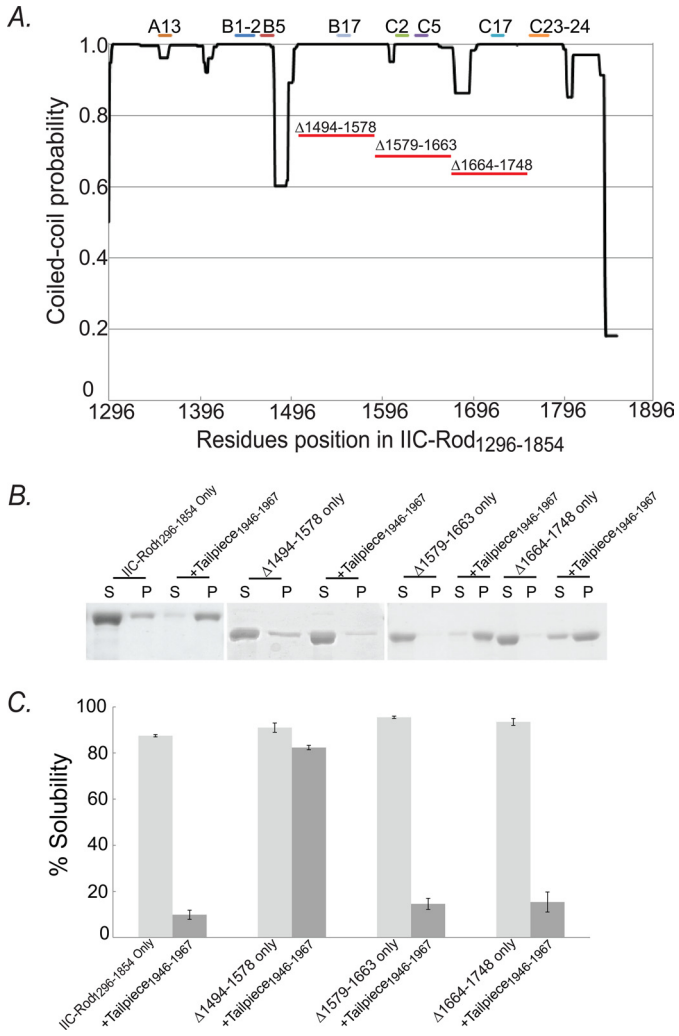

FIGURE 6. **Tailpiece binding site is important for filament assembly of IIC-Rod$_{1296-1854}$.** *A*, graph depicting the probability of IIC-Rod$_{1296-1854}$ to assume a coiled-coil confirmation as determined by COILS (33) prediction algorithm. *Bars* on *top* of the graph depict the position of the peptides that bound Tailpiece$_{1946-1967}$, and the *red lines* under the graph depict the regions deleted from rod IIC-Rod$_{1296-1854}$. *B*, 5 μM IIC-Rod$_{1296-1854}$ deletion mutants were incubated in the presence of the positively charged region of tailpiece and subjected to filament assembly assay as described in the legend for Fig. 2. *S*, supernatant; *P*, pellet. *C*, the fraction of soluble IIC-Rod$_{1296-1854}$ deletion mutants following incubation with Tailpiece$_{1946-1967}$. The extent of self-assembly was calculated as the percentage of IIC-Rod$_{1296-1854}$ containing deletions remaining in the supernatant after high speed centrifugation. The results are averages ± S.D. of three independent experiments.

(Fig. 6, *B* and *C*). When incubated with the positively charged Tailpiece$_{1946-1967}$, only IIC-Rod$_{1296-1854}^{\Delta 1494-1578}$ remained in the supernatant and was unable to form filaments (Fig. 6, *B* and *C*). In contrast, when IIC-Rod$_{1296-1854}^{\Delta 1579-1663}$ and IIC-Rod$_{1296-1854}^{\Delta 1664-1748}$ were incubated with Tailpiece$_{1946-1967}$, they retained their ability to form insoluble structures and appeared mainly in the pellet (Fig. 6, *B* and *C*). This indicates that residues 1494–1578 in the rod are required for the tailpiece ability to induce filament assembly. To assess the effect of the tailpiece binding to the rod on filament assembly, we compared the solubility of assembly-competent IIC-Rod fragments containing the entire C-terminal region including the tailpiece, in which only the putative binding sites were removed (IIC-Rod$_{1296-2000}^{\Delta 1494-1578}$, IIC-Rod$_{1296-2000}^{\Delta 1579-1663}$, and IIC-Rod$_{1296-2000}^{\Delta 1664-1748}$, Fig. 1) with similar fragments in which the tailpiece was removed (IIC-Rod$_{1296-1955}^{\Delta 1494-1578}$, IIC-Rod$_{1296-1955}^{\Delta 1579-1663}$, and IIC-Rod$_{1296-1955}^{\Delta 1664-1748}$, Fig. 1). Removing the tailpiece from wild type IIC-Rod fragment resulted in a marked decrease in filament assembly (IIC-Rod$_{1296-2000}$ *versus* IIC-Rod$_{1296-1955}$ (14) Fig. 7, *A–D*). To quantify this effect, we compared the point of 50% solubility of each mutant and plotted the change relative to the same respective mutant containing the tailpiece (Fig. 7*E*). Removing the tailpiece of IIC-Rod$_{1296-2000}^{\Delta 1579-1663}$ or IIC-Rod$_{1296-2000}^{\Delta 1664-1748}$ resulted in a decrease in filament assembly similar to that of removing the tailpiece from IIC-Rod$_{1296-2000}$ (Fig. 7*E*). These results indicate that IIC-Rods containing deletions 1579–1663 or 1664–1748 maintained the effect of the tailpiece on their solubility properties. In contrast, removal of residues 1494–1578 completely abolished the effect observed due to the absence of the tailpiece. These results indicate that residues 1494–1578 are probably the main tailpiece binding site because removing it resulted in loss of tailpiece effect on filament assembly. Because no major effect was seen for residues 1608–1642 and 1713–1775, it is possible that these sites play other roles in filament assembly.

Phosphorylation of the Tailpiece Positively Charged Region Inhibits Its Ability to Induce NMII-C Filament Assembly—Data from our laboratory and others have previously shown that both PKC and CKII phosphorylate the NMII tailpiece (8). We have previously shown that Casein kinase II phosphorylation by PKC at residues Thr^{1957} and Thr^{1960} increases the solubility properties of NMII-C *in vitro* and NMII-C cellular localization *in vivo* (15). Thus, phosphorylation allows dynamic control over NMII filament assembly *in vivo*. To better understand the mechanism by which PKC phosphorylation affects NMII-C filament assembly, we synthesized Tailpiece$_{1946-1967}$ peptides that are phosphorylated on Thr^{1957} or Thr^{1960} (Table 1) and tested their ability to induce IIC-Rod$_{1296-1854}$ filament assembly. As shown in Fig. 8*A*, phosphorylation of Thr^{1957} or Thr^{1960} completely abolished the ability of Tailpiece$_{1946-1967}$ to induce filament assembly of IIC-Rod$_{1296-1854.}$ CD analysis was used to assess the α-helical content of IIC-Rod$_{1296-1854}$ following incubation with the phospho-peptides. In contrast to WT Tailpiece$_{1946-1967}$ (Fig. 8*B*), adding either Tailpiece$_{1946-1967\text{-p}}$T^{1957} or Tailpiece$_{1946-1967\text{-p}}$T^{1960} to IIC-Rod$_{1296-1854}$ did not have any effect on the IIC-Rod$_{1296-1854}$ α-helical content (Fig. 8*B*). Together, these results indicate that phosphorylation of either Thr^{1957} or Thr^{1960} abolished its ability to promote IIC-Rod$_{1296-1854}$ filament assembly. Thus, it may be that phosphorylation of the tailpiece results in binding inhibition with subsequent decrease in filament assembly. This presents a possible mechanism explaining the role of tailpiece phosphorylation in filament assembly. PKC phosphorylates residues in the positively charged region of the tailpiece, whereas CKII phosphorylates residues in the negatively charged region of the tailpiece. Accordingly, only phosphorylation by PKC was shown to affect NMII filament assembly both *in vivo* and *in vitro* (15, 24–29), supporting our findings that the positively charged region of the tailpiece is crucial for tailpiece binding to the IIC-Rod.

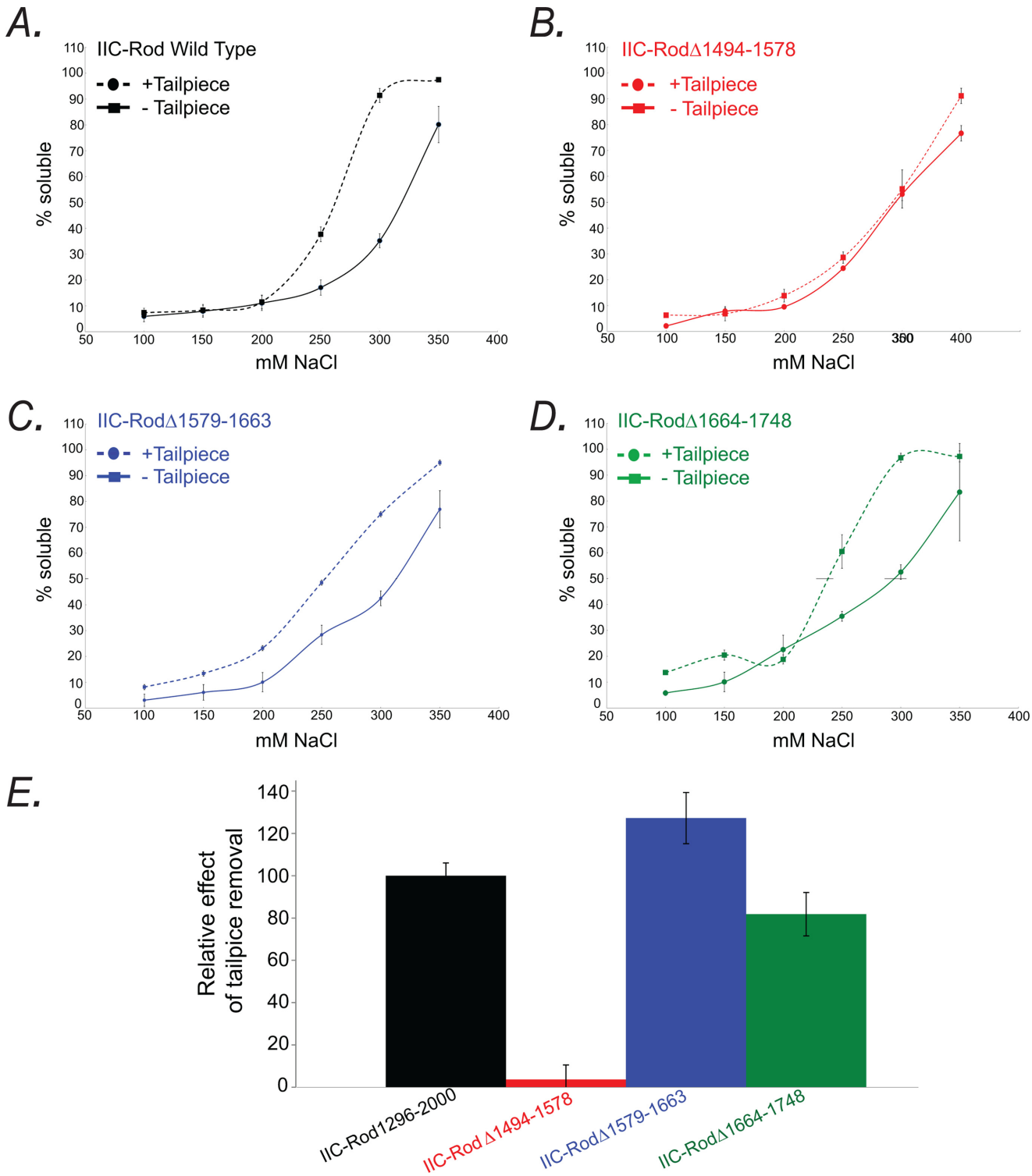

FIGURE 7. **The effect of the tailpiece removal on filament assembly of IIC-Rod fragments.** *A–D, in vitro* self-assembly of tailless NMII rod fragments. 0.1 mg/ml IIC-Rod fragments were expressed and purified from *Escherichia coli* as described (15). Proteins were dialyzed against different NaCl concentrations, and the extent of assembly was calculated as the percentage of rod fragment remaining in the supernatant after high speed centrifugation. *E*, relative effect of the tailpiece on binding site-deficient IIC-Rod fragment assembly properties. The 50% solubility point was calculated for binding site-deficient mutants containing or lacking the tailpiece. Difference is represented as the percentage relative to the wild type IIC-Rod$_{1296-2000}$ fragment. The results are averages ± S.D. of three independent experiments.

DISCUSSION

The Disordered Nature of the Tailpiece Is a Key for Binding the IIC-Rod$_{1296-1854}$—In our previous study, we showed that the positive part of tailpiece (residues 1946–1967) binds NMII-C Rod and induces its organization into the filaments (16). In the current study, we elucidated the detailed molecular interactions required for the tailpiece-induced filament assembly. Using a combination of alanine scan, sedimentation analy-

sis, and CD spectroscopy, we identified tailpiece residues Arg^{1946}, Arg^{1948}, Arg^{1950}, Arg^{1951}, Arg^{1959}, Phe^{1956}, Arg^{1962}, and Phe^{1965} to be crucial for inducing the filament assembly process. The finding that positive and aromatic residues are crucial for binding indicates that the tailpiece effect may be due to a combination of specific electrostatic and hydrophobic interactions. This is further supported by the observation that not all positive residues are crucial for binding and by the observation that the peptides did not affect the CD spectrum of the coiled-coil rod at high salt concentration. Furthermore, the crucial residues are distributed over the entire length of the positive part of tailpiece (Fig. 2). This distribution suggests that the tailpiece may fold into a specific structure upon binding to the rod, bringing all these residues to a unique orientation that favors binding. Thus, substitution of any of these residues to alanine may result in the inability of the $Tailpiece_{1946-1967}$ to fold upon binding, abolishing its ability to induce assembly. The importance of the positively charged residues for filament assembly was recently described for *Drosophila* NMII (30). However, the fact that not all of the positively charged residues have the same effect (Fig. 2), together with the distribution of these residues over the entire length of the positively charged region of the tailpiece, implies that specific interactions are needed for the binding of the tailpiece to IIC-Rod.

We have previously shown that the unbound tailpiece exists in a disordered conformation (16). Many disordered protein regions are known to fold and gain a defined structure upon ligand binding (31). This seems to be the case with the NMII-C tailpiece as well. We conclude that the disordered nature of the tailpiece is required to bring the residues that interact with the rod to close spatial proximity. This may also explain why some residues (Thr^{1957} and Thr^{1958}) retain some effect on filament assembly, albeit a low one. The observation that aromatic residues are also crucial for coiled-coil filament formation may indicate the involvement of cation-π interactions that stabilize the bound conformation of the tailpiece peptide during its interaction with $IIC\text{-}Rod_{1296-1854}$.

$Tailpiece_{1946-1967}$ Has Multiple Binding Sites in NMII-C Rod—Our peptide array screening revealed eight putative binding sites to the positive tailpiece peptide in $IIC\text{-}Rod_{1271-1954}$. These sites define five main regions that include residues 1348–1361, 1432–1473, 1544–1557, 1608–1642, and 1713–1775, indicating that the $Tailpiece_{1946-1967}$ has more than one binding site in the rod. Functional analysis of three interaction regions revealed that only deletion of residues 1494–1578 resulted in loss of tailpiece effect on $IIC\text{-}Rod_{1296-1854}$ (Fig. 6, *B* and *C*). Quantifying the effect of this deletion on $IIC\text{-}Rod_{1296-1854}$ filament assembly revealed that some residual effect was still retained as adding the tailpiece to $IIC\text{-}Rod_{1296-1854}^{\Delta 1494-1578}$ resulted in ~80% solubility when compared with the ~90% seen without the addition of the tailpiece. This result may indicate that not all the effects of the tailpiece are mediated by binding to residues 1494–1578 and hint to the existence of additional binding sites. We thus categorize the $Tailpiece_{1946-1967}$ binding sites in the rod into primary and secondary sites (Fig. 9). Deletion of primary sites causes the coiled-coil rod to lose its ability to assemble into filaments in the presence of the tailpiece. Deletion of secondary sites may cause only partial loss of filament-forming ability due to decreased interaction affinity with the tailpiece. Thus, residues 1494–1578 serve as a primary binding site,

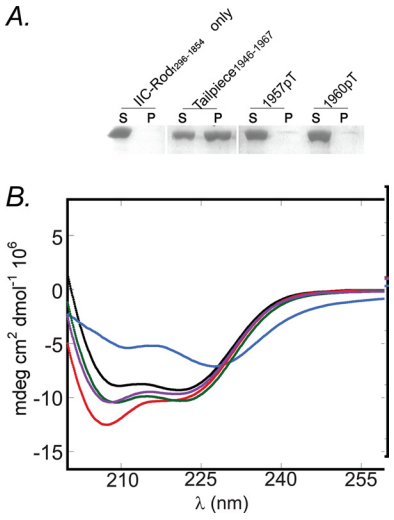

FIGURE 8. **The effect of phospho-tailpiece peptides on $IIC\text{-}Rod_{1296-1854}$ filament assembly.** *A*, 5 μM $IIC\text{-}Rod_{1296-1854}$ was incubated in the presence of 20 μM tailpiece peptides and subjected to filament assembly assay as described in the legend for Fig. 2. *S*, supernatant; *P*, pellet. *B*, CD spectra of $IIC\text{-}Rod_{1296-1854}$ with the phospho-tailpiece peptides. *Black line*, CD spectra of 0.01 mM $IIC\text{-}Rod_{1296-1854}$ alone; *blue line*, with $Tailpiece_{1946-1967}$; *red line*, $Tailpiece_{1968-2000}$; *magenta line*, $Tailpiece_{1946-1967\text{-}pT^{1957}}$; *cyan line*, with $Tailpiece_{1946-1967\text{-}pT^{1960}}$.

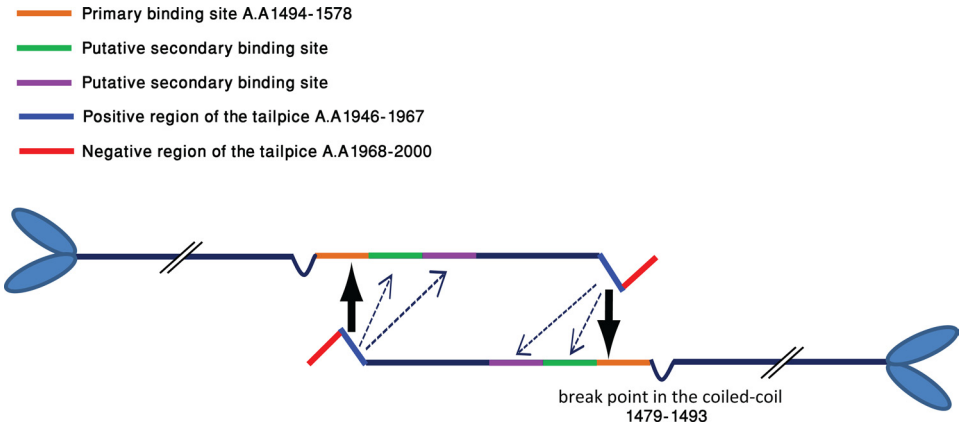

FIGURE 9. **A model depicting the modulation of NMII filament assembly by the tailpiece.** *Orange bar* and *large arrow* indicate primary site, and *green bars*, *magenta bars*, and *dashed arrows* indicate secondary sites for the binding of the tailpiece. *AA*, amino acids. See "Discussion" for more details.

whereas residues 1579–1663 and 1664–1748 are probably secondary.

Binding multiple regions within the coiled-coil rod was recently described for the assembly competence domain (30). It was proposed that interaction of this domain with multiple regions along the coiled-coil domain generates stable overlaps between myosin molecules. In our previous study, we showed that $Tailpiece_{1946-1967}$ acts like the assembly competence domain by inducing the filament assembly of a truncated coiled-coil rod fragment that was not able to form filaments on its own (16). Binding of the tailpiece to a number of sites in the coiled-coil rod may result in stronger interactions, increasing the stability of NMII-C filaments.

Tailpiece Phosphorylation Abolishes Its Interaction with the Rod—The filament assembly-disassembly equilibrium of NMII is dynamically controlled by phosphorylation *in vivo* (8). However, only the mechanism by which light chain phosphorylation enhanced NMII assembly was understood to date (8). In contrast, phosphorylation of the tailpiece results in filament disassembly in a yet unknown mechanism (8). Our results show that phosphorylation of the positively charged region renders the tailpiece unable to bind the rod. As tailpiece binding is crucial for filament assembly, inhibiting this binding results in decreased filament assembly. Data from our laboratory and others have previously shown that both PKC and Casein kinase II phosphorylate the NMII tailpiece (8). PKC phosphorylates residues in the positively charged region, whereas CKII phosphorylates residues in the negatively charged region of the tailpiece. Accordingly, only phosphorylation by PKC was shown to affect NMII filament assembly both *in vivo* and *in vitro* (15, 24–29).

Conclusions—The complexities of filament assembly control make studying specific effects *in vivo* extremely difficult. Based on our results, we propose a model for NMII tailpiece ability to modulate NMII filament assembly (Fig. 9). Binding of the positively charged region of the tailpiece at primary sites on the rod promotes filament assembly. Additional binding to secondary sites provides the fine tuning of the interaction and increases the interaction strength. This binding is dependent on both electrostatic interactions and conformational changes of the tailpiece. Phosphorylation of the positively charged region by PKC disrupts these forces, dislocating the tailpiece from the rod and removing any positive effect on filament assembly. By modulating the oligomerization equilibrium of NMII-C toward its active oligomeric state, the positively charged $Tailpiece_{1946-1967}$ acts as a "shiftide" (16, 32). Our results provide insight into how shiftides act by indicating exactly which residues are important for their activity and which molecular determinants they bind in the target protein. Understanding the forces controlling NMII dynamics has been greatly expanded in the last decade, but still much remains unsolved. Further work is needed to understand the interactions between the negatively and positively charged regions of the tailpiece. Additionally, it is still unclear whether the tailpiece promotes filament assembly by binding the rod intermolecularly or rather by creating bridges between different rod molecules in a filament. Because the tailpiece is one of the major forces controlling filament assembly *in vivo*, elucidating its functional mechanism is of great importance for future manipulation of cellular processes in which NMII participates, such as cell division and migration.

Acknowledgment—We thank Dr. Robert S. Adelstein for the NMII-C construct.

REFERENCES

1. Sellers, J. R. (1999) *Myosins*, Second Ed., Oxford University Press, Oxford
2. Conti, M. A., and Adelstein, R. S. (2008) Nonmuscle myosin II moves in new directions. *J. Cell Sci.* **121,** 11–18
3. Matsumura, F. (2005) Regulation of myosin II during cytokinesis in higher eukaryotes. *Trends Cell Biol.* **15,** 371–377
4. Lauffenburger, D. A., and Horwitz, A. F. (1996) Cell migration: a physically integrated molecular process. *Cell* **84,** 359–369
5. Sellers, J. R. (2000) Myosins: a diverse superfamily. *Biochim. Biophys. Acta* **1496,** 3–22
6. Warrick, H. M., and Spudich, J. A. (1987) Myosin structure and function in cell motility. *Ann. Rev. Cell Biol.* **3,** 379–421
7. Bresnick, A. R. (1999) Molecular mechanisms of nonmuscle myosin-II regulation. *Curr. Opin. Cell Biol.* **11,** 26–33
8. Vicente-Manzanares, M., Ma, X., Adelstein, R. S., and Horwitz, A. R. (2009) Non-muscle myosin II takes centre stage in cell adhesion and migration. *Nat. Rev. Mol. Cell Biol.* **10,** 778–790
9. Sohn, R. L., Vikstrom, K. L., Strauss, M., Cohen, C., Szent-Gyorgyi, A. G., and Leinwand, L. A. (1997) A 29 residue region of the sarcomeric myosin rod is necessary for filament formation. *J. Mol. Biol.* **266,** 317–330
10. Atkinson, S. J., and Stewart, M. (1992) Molecular interactions in myosin assembly. Role of the 28-residue charge repeat in the rod. *J. Mol. Biol.* **226,** 7–13
11. McLachlan, A. D., and Karn, J. (1982) Periodic charge distributions in the myosin rod amino acid sequence match cross-bridge spacings in muscle. *Nature* **299,** 226–231
12. Nakasawa, T., Takahashi, M., Matsuzawa, F., Aikawa, S., Togashi, Y., Saitoh, T., Yamagishi, A., and Yazawa, M. (2005) Critical regions for assembly of vertebrate nonmuscle myosin II. *Biochemistry* **44,** 174–183
13. Rosenberg, M., Straussman, R., Ben-Ya'acov, A., Ronen, D., and Ravid, S. (2008) MHC-IIB filament assembly and cellular localization are governed by the rod net charge. *PloS One* **3,** e1496
14. Straussman, R. (2005) *New insights into the assembly properties of myosin II*. Ph.D thesis, The Hebrew University of Jerusalem, Jerusalem, Israel
15. Ronen, D., and Ravid, S. (2009) Myosin II tailpiece determines its paracrystal structure, filament assembly properties, and cellular localization. *J. Biol. Chem.* **284,** 24948–24957
16. Ronen, D., Rosenberg, M. M., Shalev, D. E., Rosenberg, M., Rotem, S., Friedler, A., and Ravid, S. (2010) The positively charged region of the myosin IIC non-helical tailpiece promotes filament assembly. *J. Biol. Chem.* **285,** 7079–7086
17. Sinard, J. H., Rimm, D. L., and Pollard, T. D. (1990) Identification of functional regions on the tail of Acanthamoeba myosin-II using recombinant fusion proteins. II. Assembly properties of tails with NH2- and COOH-terminal deletions. *J. Cell Biol.* **111,** 2417–2426
18. Ikebe, M., Komatsu, S., Woodhead, J. L., Mabuchi, K., Ikebe, R., Saito, J., Craig, R., and Higashihara, M. (2001) The tip of the coiled-coil rod determines the filament formation of smooth muscle and nonmuscle myosin. *J. Biol. Chem.* **276,** 30293–30300
19. Sato, M. K., Takahashi, M., and Yazawa, M. (2007) Two regions of the tail are necessary for the isoform-specific functions of nonmuscle myosin IIB. *Mol. Biol. Cell* **18,** 1009–1017
20. Straussman, R., Ben-Ya'acov, A., Woolfson, D. N., and Ravid, S. (2007) Kinking the coiled coil – negatively charged residues at the coiled-coil interface. *J. Mol. Biol.* **366,** 1232–1242
21. Katz, C., Levy-Beladev, L., Rotem-Bamberger, S., Rito, T., Rüdiger, S. G., and Friedler, A. (2011) Studying protein-protein interactions using peptide arrays. *Chem. Soc. Rev.* **40,** 2131–2145
22. Franke, J. D., Dong, F., Rickoll, W. L., Kelley, M. J., and Kiehart, D. P. (2005) Rod mutations associated with MYH9-related disorders disrupt non-

muscle myosin-IIA assembly. *Blood* **105,** 161–169
23. McLachlan, A. D. (1984) Structural implications of the myosin amino acid sequence. *Annu. Rev. Biophys. Bioeng* **13,** 167–189
24. Murakami, N., Kotula, L., and Hwang, Y.-W. (2000) Two distinct mechanisms for regulation of nonmuscle myosin assembly via the heavy chain: phosphorylation for MIIB and mts 1 binding for MIIA. *Biochemistry* **39,** 11441–11451
25. Dulyaninova, N. G., Malashkevich, V. N., Almo, S. C., and Bresnick, A. R. (2005) Regulation of myosin-IIA assembly and Mts1 binding by heavy chain phosphorylation. *Biochemistry* **44,** 6867–6876
26. Dulyaninova, N. G., House, R. P., Betapudi, V., and Bresnick, A. R. (2007) Myosin-IIA heavy-chain phosphorylation regulates the motility of MDA-MB-231 carcinoma cells. *Mol. Biol. Cell* **18,** 3144–3155
27. Ben-Ya'acov, A., and Ravid, S. (2003) Epidermal growth factor-mediated transient phosphorylation and membrane localization of myosin II-B are required for efficient chemotaxis. *J. Biol. Chem.* **278,** 40032–40040
28. Even-Faitelson, L., and Ravid, S. (2006) PAK1 and aPKCzeta regulate myosin II-B phosphorylation: a novel signaling pathway regulating filament assembly. *Mol. Biol. Cell* **17,** 2869–2881
29. Rosenberg, M., and Ravid, S. (2006) Protein kinase Cγ regulates myosin IIB phosphorylation, cellular localization, and filament assembly. *Mol. Biol. Cell* **17,** 1364–1374
30. Ricketson, D., Johnston, C. A., and Prehoda, K. E. (2010) Multiple tail domain interactions stabilize nonmuscle myosin II bipolar filaments. *Proc. Natl. Acad. Sci. U.S.A.* **107,** 20964–20969
31. Reingewertz, T. H., Benyamini, H., Lebendiker, M., Shalev, D. E., and Friedler, A. (2009) The C-terminal domain of the HIV-1 Vif protein is natively unfolded in its unbound state. *Protein Eng. Des. Sel.* **22,** 281–287
32. Hayouka, Z., Rosenbluh, J., Levin, A., Loya, S., Lebendiker, M., Veprintsev, D., Kotler, M., Hizi, A., Loyter, A., and Friedler, A. (2007) Inhibiting HIV-1 integrase by shifting its oligomerization equilibrium. *Proc. Natl. Acad. Sci. U.S.A.* **104,** 8316–8321
33. Lupas, A., Van Dyke, M., and Stock, J. (1991) Predicting coiled coils from protein sequences. *Science* **252,** 1162–1164